International Journal of Engineering & Technology, 7 (4.3) (2018) 115-119

International Journal of Engineering & Technology

Website: www.sciencepubco.com/index.php/IJET

Research paper

Numerical Analysis of the Informational Parameters of the Magnetic Fields in the Area of the Defects of Wheel Pairs Axes

Iryna Shvedchykova[1]*, Jasim Mohmed Jasim Jasim[2], Olexandr Shevchenko[3], Iryna Soloshych[4]

[1]*Kyiv National University of Technologies and Design*
[2]*AlFurat Al Awsat Technical University – Almosaib technical college*
[3]*Volodymyr Dahl East Ukrainian National University*
[4]*Kremenchuk Mykhailo Ostrohradskyi National University*
**Corresponding author E-mail:ishved89@gmail.com*

Abstract

The article is devoted to the problem in diagnostic for axes of wheel sets of rolling stock at the railroad lines. It shows that the time counter method of magnetic powder control has low productivity and is characterized by high subjectivity and the impossibility of automating the control process. To eliminate these defects and improve the reliability for detection of defects on the surface of the stepped axis a method based on the using of fluxgate transducer is proposed. It was carried out the analysis of magnetic fields near the surface of the axles of wheel sets using the developed mathematical models, which made it possible to calculate both the defect fields and the stray field of the stepped surface of axis. Spatial and frequency selection of useful signals based on the analysis of information parameters of magnetic fields of stray of surface and subsurface defects and fields induced by the stepped surface of the magnetized axis is proved.

Keywords: *Defect; Fluxgate Transducer; Magnetic Stray Field; Magnetic Interference; Non-Destructive Testing.*

1. Introduction

The increase in the speed of passenger and freight trains poses increased requirements for safety on rail transport. Wheel pair is of the most crucial parts of the rolling stock, malfunction of which is strictly forbidden. Any defect of a wheel pair, for example, a fracture of the axis, can lead to severe consequences, which are accompanied by large economic losses, and often, human casualties.

Defects of axes of wheel pairs emerge under the influence of various factors and appear in practice with varying frequency. By origin, the defects in the axes of the wheel sets of the rolling stock are subdivided into operational and production technological [1]. Fatigue cracks are the most common operational defects. The main reason of their appearance is the influence of high variable mechanical stress. They arise, in common, in the places of stress concentration: in fillets, in places with sharp cross-sections, at the base of the thread, etc.

Industrial and technological defects arise during the manufacturing process of the axis. In this way, shells, non-metallic inclusions (particles of slag, graphite, sand, etc.) form in the process of steel production. Laminations, breakages, risks, having a variety of shapes, arise during forging and rolling. There are also defects of industrial and technological origin, such as stress concentrators and potential sources of fatigue failure in the axes of wheel sets. These defects, if they are not detected in the manufacturing process, are manifested, as a rule, at the initial moment of operation. This makes them especially dangerous, as it inevitably leads to the development of obsolete cracks. The axes of wheel sets with cracks in the under-hull, pre-intermediate and middle parts, as well as on the necks and fillets of the axle are not allowed for operation.

Thus, the wheel pair is the main unit of the rolling stock and is most susceptible to dynamic loads. Therefore, the testing of the state of a wheel pair and, first of all, its axis, is an actual scientific and technical task.

2. Problem Statement

For the timely detection and removal of axle of wheel pairs with defects in the manufacturing and repair process, visual inspections are provided, as well as the use of technical means of magnetic, ultrasonic or eddy current flaw testing [1]. At the same time, the magnetic particle method of non-destructive testing is mandatory. This method is used, both in the production of axes, and in the process of their operation; it differs in the simplicity of implementation and visibility of the results of control. However, the magnetic powder method of pinning the following significant drawbacks: low productivity, subjectivity in the evaluation of testing results and the inability to automate the control process. The magnetic fluxgate (fluxgate) method allows to completely automate the testing process, which becomes more rapid and effective in stationary and non-stationary diagnostic conditions.

The fluxgate testing method is based on the detection of a defect in the magnetized product by fluxgate transducer of the magnetic field and converting it into an electrical signal. Fluxgate magnetometers are a class of sensitive sensors used to measure direct current or low-frequency magnetic field vectors. Conventional fluxgate sensors typically feature low noise, high sensitivity and excellent accuracy [2, 3].

Fluxgate transducers are promising in applications for military detection, inertial navigation, bio-medical identification [4, 5] and non-destructive testing [6]. Due to the trend of system miniaturization, the development of miniature fluxgate sensors compatible

with complementary metal-oxide-semiconductor and micro-electromechanical systems technologies has been emerging in recent years. Also promising is the use of new materials, for example, based on nanoferrite, in the manufacture of cores of fluxgate sensors [7]. One of the directions of the use of fluxgate sensors is also the control of damages of rotor rods of asynchronous motors [8].

The fluxgate method has not yet found wide application in testing the axes of wheel pairs, because of the complex geometric shape of the axis. The presence of a high level of interference in the form of magnetic scattering fields from magnetized steps and the edges of the axis with a high gradient precluded the possibility of monitoring by existing fluxgate defectoscopes. At the same time, sensitivity, production and automation capabilities make this method more preferable. Theoretical and experimental studies are needed, as well as the development of new methods and technical means of the fluxgate testing that would enable continuous monitoring of axle defects during their manufacture and operation.

The purpose of the paper is to numerically analyze the information parameters of the magnetic field of scattering of the wheel pair axis and the magnetic field of the interference to substantiate the possibility of selecting interference caused by the stepped surface of the axis.

3. Mathematical Model of Informational Magnetic Fields

To achieve the goal, it is necessary to develop mathematical models of defect stray fields, as well as a mathematical model of the magnetic field induced by the magnetized wheel pair axis (interference fields).

3.1. Mathematical Model of Magnetic Stray Field of Defects

A large number of mathematical models of magnetic stray fields are known for various geometric shapes of defects [9]. All of them have common drawbacks: either they are constructed with a significant idealization of the original problem (the three-dimensional nature of the field is not taken into account), or they are highly labour intensity in calculations.

The defect in the object has finite dimensions, so its informational stray field is three-dimensional. Mathematical model of the field of the magnetization vector in a nonlinear ferromagnetic medium was developed taking into account the three-dimensionality of the field. This will improve the accuracy of calculations and reduce the complexity of calculations.

In this paper, as a calculation method, a method based on the removal of magnetic charges on the surface of a ferromagnetic material is adopted. The follow integral equation is used as an initial mathematical model for calculating magnetic intensity $\overline{H}_i$ of three-dimensional defects magnetic stray fields [10]

$$\overline{H}_i = \frac{1}{4\pi}\sum_{j=1}^{N}\sum_{k=1}^{6}\int_{S_k}\frac{\left[\overline{M}_{jk}(H)\cdot\overline{1}_n\right]\cdot\overline{1}_r}{r^2_{ji}}dS_{jk} + \overline{H}_0, \quad (1)$$

where $i = \overline{1,N}$; i, j – points of observation and source of the field, respectively; r_{ji} – module of the radius-vector from the source point j into point of observation i; $\overline{H}_0$ – intensity vector of magnetized field; S_k –area of a section of ferromagnetic material with a defect; $\overline{M}_{jk}(H)$ – magnetization of ferromagnetic medium; N – number of elementary volumes, which are parallelepipeds with the number of faces k (k = 6) into which the region of the ferromagnetic material is divided.

The following assumptions are made under the adaptation the mathematical model (1) to the problem:

- the magnetizing field in the area where the defect is located is assumed as uniform, since the dimensions of the defect are many times smaller than the diagnosed part;
- the curvature of the surface of the axis is not taken into account because of the small geometric dimensions of the defect in comparison with the radius of the axis.

In the calculations according to the formula (1), the hysteresis loop of the ferromagnetic material of the axis was approximated by the following analytical dependence

$$M^{\pm} = \frac{M_s}{\pi}\left[2arctg\frac{\pi}{2}\left(\frac{H \pm H_c}{H_s}\right) \pm \left(arctg\frac{\pi}{2}\frac{H_m + H_c}{H_s} - arctg\frac{\pi}{2}\frac{H_m - H_c}{H_s}\right)\right], \quad (2)$$

where H_c, H_s – coercive force and intensity of saturation, respectively; M_s – magnetization of saturation; H_m – maximum value of field intensity.

By integrating expression (1), formulas for calculating at the point i the field intensity $\overline{H}_i$ created by an elementary volume located at point j having a magnetization $\overline{M}_j$ are obtained

$$\begin{aligned}
&\overline{H}_i = \overline{1}_x H_x + \overline{1}_y H_y + \overline{1}_z H_z,\\
&H_x = H_x^{/} + H_x^{//} + H_x^{///},\\
&H_y = H_y^{/} + H_y^{//} + H_y^{///},\\
&H_z = H_z^{/} + H_z^{//} + H_z^{///}.
\end{aligned} \quad (3)$$

where x, y, z – coordinates of a rectangular Cartesian coordinate system. For all components H_x, H_y, H_z of field intensity $\overline{H}_i$ the calculated expressions were obtained.

Therefore, the calculated expressions for the component H_x ($H_x^{/}$, $H_x^{//}$, $H_x^{///}$) of magnetic field intensity vector $\overline{H}_i$ are presented below as an example:

for $H_x^{/}$ component -

$$H_x^{/} = \frac{1}{4\pi}\sum_{k=1}^{8} M_k arctg\frac{(z_j - z_i + \Delta w_k)(y_j - y_i + \Delta v_k)}{(x_j - x_i + \Delta u_k)R_k}, \quad (4)$$

$$R_k = \sqrt{(x_j - x_i + \Delta u_k)^2 + (y_j - y_i + \Delta v_k)^2 + (z_j - z_i + \Delta w_k)^2}, \quad (5)$$

where values $M_k, \Delta u_k, \Delta v_k, \Delta w_k$ are defined as follows

$$\begin{aligned}
&\begin{cases} k = 1,4,6 & M_k = M_x; \\ k = 2,3,5 & M_k = -M_x; \end{cases} \qquad \begin{cases} k = 1,2,3,4 & \Delta u_k = \Delta x; \\ k = 5,6 & \Delta u_k = -\Delta x; \end{cases}\\
&\begin{cases} k = 1,2,5,6 & \Delta v_k = \Delta y; \\ k = 3,4 & \Delta v_k = -\Delta y; \end{cases} \qquad \begin{cases} k = 1,3,5 & \Delta w_k = \Delta z; \\ k = 2,4,6 & \Delta w_k = -\Delta z; \end{cases}
\end{aligned} \quad (6)$$

for $H_x^{//}$ component -

$$H_x^{//} = \frac{1}{4\pi}\sum_{k=1}^{8}\frac{M_k}{2}\ln\left|z_j - z_i + \Delta w_k + R_k\right|, \quad (7)$$

where values $M_k, \Delta u_k, \Delta v_k, \Delta w_k$ are defined as follows

$$\begin{cases} k = 1,4,6 & M_k = M_y; \\ k = 2,3,5 & M_k = -M_y; \end{cases} \qquad \begin{cases} k = 1,2,5,6 & \Delta u_k = \Delta x; \\ k = 3,4 & \Delta u_k = -\Delta x; \end{cases} \quad (8)$$

$$\begin{cases} k=1,2,3,4 & \Delta v_k=\Delta y; \\ k=5,6 & \Delta v_k=-\Delta y; \end{cases} \qquad \begin{cases} k=1,3,5 & \Delta w_k=\Delta z; \\ k=2,4,6 & \Delta w_k=-\Delta z; \end{cases}$$

for H_x''' component -

$$H_x''' = \frac{1}{4\pi}\sum_{k=1}^{8}\frac{M_k}{2} ln\left|y_j - y_i + \Delta v_k + R_k\right|. \qquad (9)$$

Values $M_k, \Delta u_k, \Delta v_k, \Delta w_k$ in expression (9) are defined as follows

$$\begin{cases} k=1,4,6 & M_k=M_z; \\ k=2,3,5 & M_k=-M_z; \\ k=1,3,5 & \Delta v_k=\Delta y; \\ k=2,4,6 & \Delta v_k=-\Delta y; \end{cases} \qquad \begin{cases} k=1,2,5,6 & \Delta u_k=\Delta x; \\ k=3,4 & \Delta u_k=-\Delta x; \\ k=1,2,3,4 & \Delta w_k=\Delta z; \\ k=5,6 & \Delta w_k=-\Delta z. \end{cases} \qquad (10)$$

In expressions (6), (8), (10): Δx, Δy, Δz – geometric dimensions of edges of elementary volumes in the form of parallelepipeds, into which the investigated region is divided; M_x, M_y, M_z – projections on the axis 0*x*, 0*y*, 0*z*, respectively, of the magnetization M_k of the *k* face of the elementary volume.

Thereby, on the basis of nonlinear vector integral equations, the model (formula (3)) for calculating the three-dimensional information field of defect scattering taking into account the nonlinear properties of the material and the features of the geometry of the defects is proposed.

3.2. Mathematical Model of Magnetic Field of Magnetized Axis (Magnetic Field of Interference)

To calculate the magnetic field of the interference, it is necessary to calculate the magnetic field near the surface of the magnetized axis. It is assumed that the source of the magnetic field is the magnetization $\overline{M}$ at the ends of the axis (Figure 1). The value of this magnetization can be determined using the theory of nonlinear magnetic circuits.

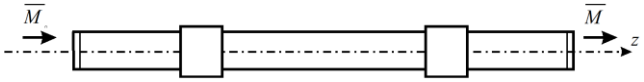

Fig. 1: The model of magnetic field source of magnetized axis

To determine the magnetization $\overline{M}$ at the ends of the axis, simplified equivalent scheme of magnetic circuit (Figure 2) has been developed without taking into account the stray fluxes. The magnetic circuit includes the investigated axis and the core of the magnetizing device. In the scheme they are represented by the following nonlinear magnetic resistances:

R_{01}, R_{02} – magnetic resistance of sections of the wheel pair axis;

R_b – magnetic resistance of air gaps between the core of the magnetizing device and the axis;

R_c – magnetic resistance of the core of the magnetizing device.

In Figure 2 the magnetomotive force of the magnetizing device is indicated as *IW*.

A lumped magnetic circuit method was used for the calculation of magnetic flux in ferromagnetic material taking into account the nonlinear dependence *B(H)*.

After calculation the flux Φ, the magnetic flux density *B* and the magnetization M were determined at the ends of the wheel pair axis accordingly to the following formula

$$M = \frac{1}{\mu_0}B - H, \qquad (11)$$

where H – magnetic field intensity at the ends of the axis; μ_0 – permeability of vacuum.

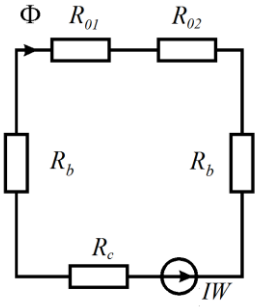

Fig. 2: Simplified equivalent scheme of magnetic circuit

Thus, it is assumed that at the ends of the axis of the wheel pair there are thin disks with a magnetization vector $\overline{M}$, which has only *z*-component. The field is calculated by solving the integral equation (1). Only in this case the elementary volumes are rings, so the calculation is carried out in a cylindrical coordinate system. The entire volume of the axis is divided into elemental volumes, the form of which is shown in Figure 3.

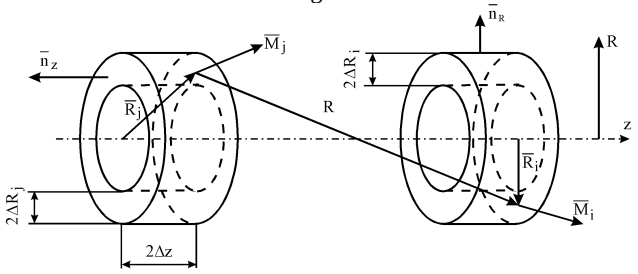

Fig. 3: View of elementary volumes

The integrals included in the sum of formula (1) will be written as follows.

For a lateral surface, the field intensity $\overline{H}_{side}$ created by the surface density of magnetic charges is equal

$$\overline{H}_{side} = grad_i \frac{1}{2\pi}\int_{-\Delta z}^{\Delta z}\int_{0}^{\pi}\frac{M_p(R_j+\Delta R_j)}{[(R_j+\Delta R_j)^2+R_j^2+(z_j-z_i)^2-2(R_j+\Delta R_j)^2R_i\cos\alpha_j]^{\frac{1}{2}}}\times$$
$$\times d\alpha_j dz_j - grad_i \frac{1}{2\pi}\int_{-\Delta z}^{\Delta z}\int_{0}^{\pi}\frac{M_p(R_j-\Delta R_j)}{[(R_j+\Delta R_j)^2+R_j^2+(z_j-z_i)^2-2(R_j-\Delta R_j)^2R_i\cos\alpha_j]^{\frac{1}{2}}}\times\times d\alpha_j dz_j. \qquad (11)$$

At the same time it is considered that $\alpha_i = 0$; $\overline{M}\cdot n_p = M_P$; $\overline{M}\cdot n_z = M_z$.

For the end-surface of the unit volume the field intensity $\overline{H}_{front}$ created by the surface density of the magnetization vector $\overline{M}$ can be obtained from the following expression

$$\overline{H}_{front} = grad_i \frac{1}{2\pi}\int_{-\Delta R_j}^{\Delta R_j}\int_{0}^{\pi}\frac{M_z R_j}{\sqrt{R_i^2+R_j^2+(z_j-z_i+\Delta z_i)^2-2R_jR_i\cos\alpha_j}}d\alpha_j dR_j -$$
$$- grad_i \frac{1}{2\pi}\int_{-\Delta R_j}^{\Delta R_j}\int_{0}^{\pi}\frac{M_p R_j}{[R_i^2+R_j^2+(z_j-z_i+\Delta z_i)^2-2R_jR_i\cos\alpha_j]^{\frac{1}{2}}}d\alpha_j dR_j. \qquad (12)$$

Thus, the magnetic field of interference can be calculated by determining the magnetization in the volume of the axis, by dividing it into elemental volumes and with following solution of the integral equation (1).

4. Results of Research

The developed mathematical models of the magnetic fields of defects stray and the magnetized axis of wheel pairs made it possible to carry out numerical experiments and to calculate the fields arising from the stepped surface of the axis, which are considered interference fields, as well as the stray fields of defects. Numerical calculations make it possible to determine methods for interference filtration.

On the first step the calculation of magnetic field of defects stray in the form of crack was performed. Geometrical model of crack-defect is shown in Figure 4, where: $2b$ – defect width; h_1, h_2 – distance, respectively, from the upper and lower boundaries of the defect to the surface of the axis; d – diameter of the testing object. The calculation was carried out for both the subsurface and surface defects (h_1 =0).

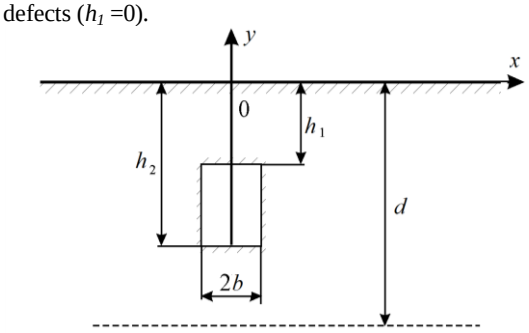

Fig. 4: Geometrical model of crack-defect

Figure 5 shows the calculated vertical components H_y of the vector $\overline{H}_i$ of the magnetic field intensity for the following defects:

- surface defect in the form of infinitely long crack by width $2b$ (b=0,005, 0,025, 0,05, 0,25, 0,5 mm) and depth h =2,5 mm (h_1 =0, $h_2 = h$) at $H_o = 2 \cdot 10^5$ A/m (Figure 5, A);
- subsurface defect by width $2b$ (b=0,05, 0,25, 0,5 mm) and h_1 =2,5 mm, h_2 = 12,5 mm (Figure 5, B).

(A)

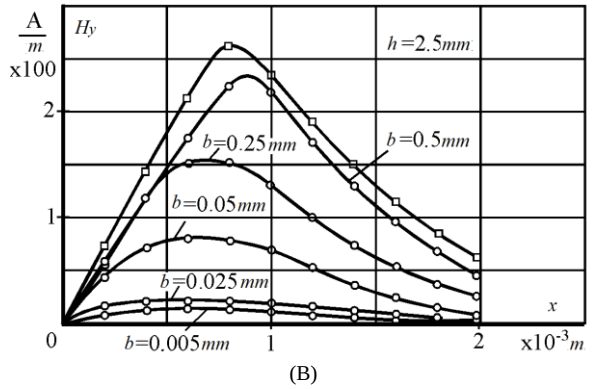

(B)

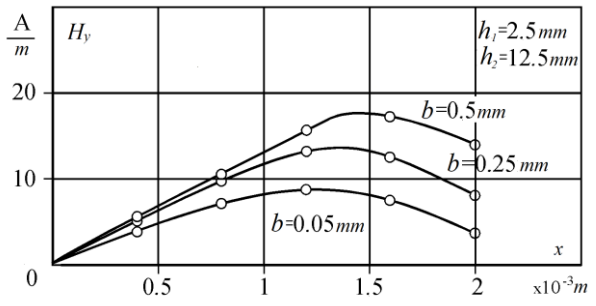

Fig. 5: Vertical components H_y of vector intensity of magnetic stray field for: (A) superficial defect; (B) subsurface defect

As follows from Figure 5, subsurface defects have lower field intensity (up to 20 A/m) and higher distance than surface ones. Practically subsurface defects, which are less than 2 mm in opening, are very difficult to detect by the fluxgate transducer at depths of up to 10 mm, since the maximum value of their field intensity does not exceed 3-12 A/m. To detect subsurface defects, it is necessary to increase the value of the magnetic field intensity of magnetization.

In the next stage, numerical experiments were carried out that made it possible to calculate the fields arising from the non-smoothness of the axis surface with given dimensions, which are considered as interference fields.

The calculation of the magnetic field of interference is based on the following assumptions:

- the axis is magnetized in a closed magnetic circuit uniformly throughout the volume to the value of the magnetization $M = 2 \cdot 10^4$ A/m corresponding to the residual magnetization;
- only one vertical (normal) component of the field intensity vector is calculated, since it is difficult to measure the tangential component on the stepped axis surface.

Figure 6 shows the calculated graph of the distribution of the normal component H_n of the magnetic field intensity along the coordinate axis 0z at a distance of 2 mm from the surface of the test object. It can be seen from the graph that the intensity H_n of the interference field changes abruptly at the steps of the shaft. In this case, the value of the modulus of the normal component of H_n varies between 480 and 710 A/m.

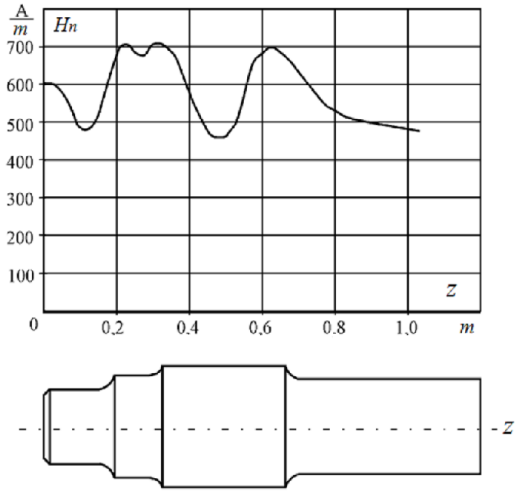

Fig. 6: Distribution of normal component H_n of magnetic field intensity over the surface of wheel pairs axis

To test the correspondence between the results of numerical analysis and the real conditions of application of the fluxgate, an experiment was carried out. The field near the surface of the magnetized axis of the wheel pair was measured. The task of the experiment was to determine how much the calculated noise field differs from the mean value of the field determined experimentally, and also how the actual field of the interference differs from the calculated one.

Since the field has been measured by fluxgate transducer connected through a gradientometric scheme, the difference ΔH_n of the vertical component of the field strength vector was calculated at points spaced from each other by a distance equal to the distance between the cores of the fluxgate. The results of experimental studies on the determination of the difference in the normal component of the magnetic field intensity vector ΔH_n in comparison with the calculated ones are given in Figure 7, where the solid lines show the dependences obtained as a result of theoretical calculations, and the dotted lines show the dependencies obtained as a result of the experiment. The discrepancy between the results of the calculations and the experiment was no more than 7%.

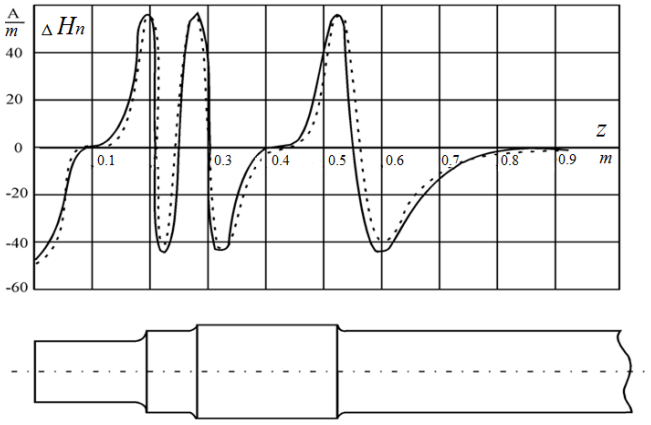

Fig. 7: The dependence of the difference component of the intensity ΔH_n at the surface of the magnetized axis in comparison with experiment

To carry out experimental studies of the defect stray fields, an installation was developed that consisted of a fluxgate magnetometer, a magnetization device, recording equipment, and instruments for calibrating a fluxgate meter [11]. The bars from steel, which is used for the preparation of axes of wheel sets, were used as samples. The coercive force of the magnetic material of the samples was H_c=1440 A/m, the dimensions of the bars were 60x100x100 mm. Simulation of defects in the samples was carried out by cutting out the rectangular grooves by an electric spark method along the entire width of the bar. Tests were carried out for samples with the following defects parameters: h=0,5; 1,0, 2,5 mm; 2b=0,2; 0,3; 0,5 mm.

The discrepancy between the results of theoretical calculations of the stray fields of surface defects of wheel pairs and experimental data did not exceed 6%. It should be noted that the main reason for the discrepancy between the theoretical studies and the experimental data is the inaccurate determination of the magnetization in the samples, since the empirical formulas were used in calculating the demagnetization coefficient.

Thus, in the process of the research it was established that over the surface of the axis, with its longitudinal magnetization, there is a field caused by a stepped surface of the axis. This field is interference. The magnitude of the field intensity of the defect stray is much smaller than the intensity of the interference field (for example, for a surface defect, it is 2-3 times less than the field intensity of the interference). However, the field of stray of defects (surface and subsurface) is much smaller in the length of the interference field.

5. Conclusion

To solve the crucial problem of increasing the efficiency of magnetic diagnostics of wheel pairs, a complex of mathematical models of the magnetic field has been developed, taking into account the nonlinear characteristics of the medium. Numerical analysis of the magnetic field using the developed models has shown that over the surface of the axis, when it is longitudinal magnetized; there is a stray field or an interference field caused by its stepped surface. The magnitude of the field intensity modulus is in the range of 480-710 A/m; the gradient of this field reaches a value of $2 \cdot 10^4$ A/m².

When calculating the stray fields of defects, it is established that the subsurface defects have a lower intensity (up to 20 A/m) and a higher distance than the surface ones. To increase the probability of detecting subsurface defects, it is necessary to increase the magnetization field intensity $(1{,}2-1{,}5)\cdot 10^6$ to A/m. Experimental research of fluxgate transducer confirms the results of theoretical calculations.

Analysis of the information parameters of stray fields showed that the spatial spectra of stray fields of defects and noise caused by a stepped surface of the axis do not overlap each other. The amplitude of the function $\Delta H(z)$ for the interference and for the useful signal is of the same order, but the rate of change of the field gradient of the magnetized axis is more than an order of magnitude lower than the rate of change of the gradient of the defect field. Therefore, it is possible to isolate the signal against a background noise. In order to increase the efficiency of the separation of a useful signal from interference during testing of the axis, it is necessary, in addition to spatial filtration, which is based on the gradientometric method of incorporating the fluxgate transducer windings, to produce digital filtration. In this case, the level of interference can be reduced by 25-30 times.

Thus, based on the results of theoretical and experimental studies, it has been established that an increase in the efficiency of diagnostics of such a critical unit as the axis of the wheel pair can be performed by replacing the magnetic particle testing with a fluxgate detector. This will improve the performance and reliability of testing.

References

[1] Ostanin SN, "Malfunctions of wagon wheel pairs and their elements", *Vagonny park*, No. 9-10(102-103), (2015), pp. 32-36, available online: http://nbuv.gov.ua/UJRN/vagpark_2015_9-10_8.

[2] Lenz J, Edelstein SL, "Magnetic sensors and their applications", *IEEE Sensors Journal*, Vol. 6, Issue 3 (2006), pp. 631-649.

[3] Lu CC, Huang J, Chiu PK, Chiu SL, Jeng JT, "High-Sensitivity Low-Noise Miniature Fluxgate Magnetometers Using a Flip Chip Conceptual Design", *Sensors* , No. 14 (2014), pp. 13815-13829.

[4] Primdahl F, "The fluxgate mechanism, part I: The gating curves of parallel and orthogonal fluxgates", *IEEE Trans. On Magn*., No. 6 (1970), pp. 376-383.

[5] Dolabdjian C, Saez S, Toledo AR, Robbes D, "Signal-to-noise improvement of bio-magnetic signals using a flux-gate probe and real time signal processing", *Rev. Sci. Instrum*., No. 69 (1998), pp. 3678-3680.

[6] David C, Marina D.-M, Lucas P, Claudio A, "Small fluxgate magnetometers: Development and future trends in Spain", *Sensors*, No. 10 (2010), pp. 1859–1870.

[7] Shynkarenko, OV, Kravchenko SA, "Surface Plasmon Resonance Sensors: Methods of Surface Functionalization and Sensitivity Enhancement", *Theoretical and Experimental Chemistry*, Vol. 51, No. 5 (2015), pp. 265–283.

[8] Romachykhina Z, Kalinov A, Qawaqzeh MZ, "Analysis of the electromagnetic field of an induction motor with broken rotor bars", *Proceedings of the International Conference on Modern Electrical and Energy System (MEES)*, (2017), pp. 112-115.

[9] Bezkorovaynyy V, Ivanovskij P, Yakovenko V, "Mathematical modeling of magnetic stray fields defects ferromagnetic products", *TEKA Commission of Motorization and Energetics in Agriculture*, Vol. 13, No.4 (2013), pp. 25-32.

[10] Tozoni OV, Maeragojz ID, *The calculation of three-dimensional electromagnetic fields*, Kiev, Tekhnika (1974), p. 352.

[11] Shvedchikova IA, Shevchenko AI, Putkaradze NL, "The experimental setup for the study magnetic stray fields of defects of ferromagnetic items", *Visnik of the Volodymyr Dahl East Ukrainian National University*, No.3 (2017), pp. 246-251.